

COMPACT TWO-LAYER MICROSTRIP BANDPASS FILTERS USING BROADSIDE-COUPLED RESONATORS

S. Vegesna and M. Saed*

Department of Electrical and Computer Engineering, Texas Tech University, Lubbock, Texas 79409, USA

Abstract—This paper presents a design methodology for realizing broadside-coupled microstrip bandpass filters on multilayer substrates to reduce the size of the filter. The new filter configuration consists of broadside coupled split-ring resonators on two layers backed by a ground plane. With the proposed new method, miniaturization to a greater extent can be achieved compared to the conventional method of realizing microstrip multilayer filters. In addition, coupling apertures in the ground plane used to achieve coupling among the resonators in conventional multilayer structures are eliminated. The proposed design is more flexible compared to traditional multilayer filters. Layers can be easily added to increase the filter order. To demonstrate the method, a miniaturized two-layered bandpass filter centered at 728 MHz with low insertion loss is implemented and investigated. Miniaturization of more than 25% is achieved compared to the conventional broadside coupled structure and more than 40% miniaturization compared to the edge coupled structure. The new microstrip filter discussed in this paper can be realized using simple fabrication techniques.

1. INTRODUCTION

Multilayer filters play an important role in modern communication systems where there is huge demand for compact filters with better selectivity and to reduce the circuit size and cost and enhance the system performance. The use of multilayer circuit configurations makes the microwave circuits more compact and the design more flexible [1]. Due to the development of modern fabrication technology, planar

Received 17 October 2011, Accepted 1 December 2011, Scheduled 8 December 2011

* Corresponding author: Mohammad Saed (mohammad.saed@ttu.edu).

microwave filters can be stacked vertically to reduce the overall circuit size instead of horizontally in conventional filters [2]. Traditional multilayer bandpass filters are designed either using apertures in the ground plane or using vias between the resonator layers using LTCC or MMIC technologies [1–11]. In [3], a multilayer bandpass filter is designed using open-loop resonator and extra metallic patches are used to achieve coupling between the two conductive layers. Even though, the structure is a two-layered filter, the circuit size is same as that of the standard edge-coupled cross-coupled resonator of same order and there is no miniaturization. In [4], two-layered broadband bandpass filter is realized using hair-pin resonators. The multilayer filter proposed in this paper is narrowband and achieves greater size reduction. In [5–9], using the ground-plane aperture technique conventional coupled resonators are used to realize different filter configurations based on the position of the coupling apertures. The apertures in the ground plane are used to achieve coupling between the resonators. In [5, 6], a four-pole bandpass filter was realized using open-loop resonators and miniaturized hairpin resonators with apertures on the common ground plane using LTCC technology to achieve coupling among the resonators with an insertion loss of 4.2 dB and passband return loss of 12 dB. In [7, 8], two-layered bandpass filter was designed using open-loop resonators and capacitively loaded square open-loop resonator with different coupling apertures for electric coupling and magnetic coupling between the resonators to achieve coupling among the resonators. The position of the coupling apertures in the ground plane plays an important role in determining the coupling factor and the type of frequency response. In [9], resonators are arranged on both sides of a common ground plane with interconnects between the layers where the coupling occurs through slots in the ground plane using MMIC technology. In [10, 11], vias are used to interconnect resonators in different layers to achieve coupling between the resonators.

The main contribution of this paper is to make use of broadside coupled resonators [12] in multilayer technology to achieve miniaturization to a greater extent, without the use of ground planes with apertures or vias. The resonator on one layer is 180° inverted with respect to the resonator in another layer and achieve coupling without any apertures in the ground plane. Using broadside coupled resonators reduces the resonant frequency to much lower frequency as opposed to using conventional multilayer resonators resulting in further miniaturization. The proposed method eliminates the need for having apertures in the ground plane since a slight misalignment of the position of the apertures in the ground plane effects the coupling as well as frequency response. The bandpass filter designed using

the proposed method makes the design more flexible compared to the conventional multilayer filters. Additional layers can be added easily to improve selectivity by increasing the order of the filter. The choice of the resonator plays an important role for realizing a compact filter. Sub-wavelength structures such as open-loop resonators, split-ring resonators (SRRs), miniaturized hair-pin resonators and other microstrip structures have been successfully used to design compact filters at microwave frequencies [5, 13–23], since these resonators can be designed with dimensions much smaller than the signal wavelength at their resonant frequency. Broadside coupled split-ring resonators with cross coupling are chosen to serve the purpose of implementing the multilayer filter compared to the conventional split-ring resonators [12] to eliminate the cross-polarization effects [24] and to realize miniaturized structures. In order to improve the selectivity of the bandpass filter, cross-coupling is introduced among the resonators to achieve elliptic function response with a pair of attenuation pole at finite frequencies, thereby improving selectivity [25]. In order to demonstrate the level of miniaturization, two structures: 1) the edge-coupled filter and 2) the proposed two layered broadside coupled filter are designed with the same coupling coefficient matrix and comparison between the two structures is done. This paper is organized as follows. In Section 2, the edge-coupled bandpass filter using split-ring resonators (EC-SRRs) is realized and simulation results as well as the measured results for the designed edge-coupled filter are presented. In Section 3, the design method for the proposed two-layered broadside-coupled filter is presented along with comparison between the measured and simulated frequency response of the filter. Various bandpass filter structures are compared with the proposed filter to demonstrate miniaturization. Finally, conclusions of this paper are presented in Section 4.

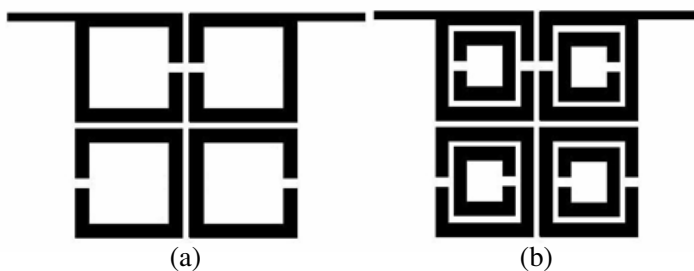


Figure 1. Four-pole edge coupled filter using (a) open-loop resonators, (b) split-ring resonators.

2. DESIGN OF EDGE-COUPLED BANDPASS FILTER

The basic design idea for the four-pole edge-coupled bandpass filter with cross-coupling is shown in Figure 1. In [25], open-loop resonators are used to realize a cross-coupled filter shown in Figure 1(a). The resonant frequency of the structure can be reduced by using split-ring resonators instead of open-loop resonators and better miniaturization can be achieved with the structure shown in Figure 1(b).

The physical dimensions of the structure determine the resonance frequency and the dimensions of the filter are determined based on the method of extracting external quality factor and from the coupling coefficient matrix [19]. Based on the knowledge of the coupling coefficient matrix, external quality factor and following the traditional design procedure, the resultant filter structures are simple and easy to realize. Cross-coupled resonators are preferred to achieve more advanced filter responses such as elliptic filters with higher selectivity and sharp cutoff since coupling exists between non-adjacent resonators [19]. The method of extracting coupling coefficients and external quality factor is used to realize the filter structure with the aid of an electromagnetic (EM) simulator. The commercial software Ansoft Designer was used for all simulations in this work. The simulator is used to find the two resonant peaks of the loosely coupled resonators for three types of coupling: electric, magnetic and mixed coupling. Due to coupling between the resonators, each resonator pair shows two resonant peaks with corresponding resonant frequencies f_1 and f_2 . Let f_1 be the lower resonant frequency and f_2 be the higher resonant frequency and the coupling coefficient for each case is calculated from the two resonant peak frequencies f_1 and f_2 and is given by [19]:

$$k = \frac{f_2^2 - f_1^2}{f_2^2 + f_1^2} \quad (1)$$

where k represents the coupling coefficient between the resonators. The design parameters of the edge-coupled filter using split-ring resonators 1–4 are shown in Figure 2.

The element values of the low-pass prototype are obtained for $\Omega = 1.8$, where Ω is frequency locations of pair of attenuation poles using the design equations given below [19]:

For $n = 4$:

$$\begin{aligned} g_1(\Omega) &= 1.22147 - 0.35543\Omega + 0.18337\Omega^2 - 0.0447\Omega^3 + 0.00425\Omega^4 \\ g_2(\Omega) &= 7.22106 - 9.48678\Omega + 5.89032\Omega^2 - 1.65776\Omega^3 + 0.17723\Omega^4 \\ J_1(\Omega) &= -4.30192 + 6.26745\Omega - 3.67345\Omega^2 + 0.9936\Omega^3 - 0.10317\Omega^4 \\ J_2(\Omega) &= 8.17573 - 11.36315\Omega + 6.96223\Omega^2 - 1.94244\Omega^3 + 0.20636\Omega^4 \end{aligned} \quad (2)$$

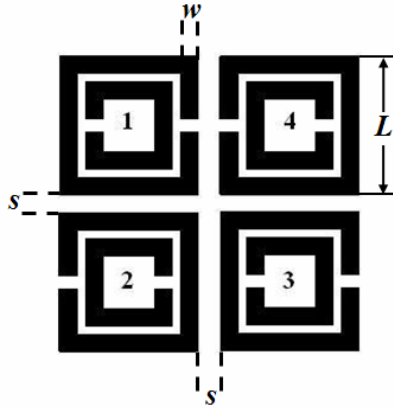


Figure 2. Four-pole cross-coupled structure using split-ring resonators. L is the side length of the resonator, s is the space between the resonators and w is the conductor width.

where g_i and J_i are capacitance of the lumped capacitor and characteristic admittance of the inverter, respectively. The g_i values are found to be $g_1 = 0.9597$, $g_2 = 1.4219$ and J_i values are found to be $J_1 = -0.2109$ and $J_2 = 1.1177$. The design parameters of the bandpass filter, i.e., the coupling coefficients and external quality factor can be determined in terms of low-pass prototype filter parameters (g_1, g_2, J_1 and J_2) and the relationship between the bandpass design parameters and the low-pass parameters are determined using the formulas below [19].

$$\begin{aligned}
 Q_{e1} &= Q_{eo} = \frac{g_1}{FBW} \\
 M_{i,i+1} &= M_{n-i,n-i+1} = \frac{FBW}{\sqrt{g_i g_{i+1}}}, \quad \text{for } i = 1 \text{ to } m - 1 \\
 M_{m,m+1} &= \frac{FBW \cdot J_m}{g_m} \\
 M_{m-1,m+2} &= \frac{FBW \cdot J_{m-1}}{g_{m-1}}
 \end{aligned} \tag{3}$$

where FBW is the fractional bandwidth, M_i 's are the coupling coefficients between the resonators, Q_{ei} and Q_{eo} are the input and output external quality factors.

For the cross-coupled filter shown in Figure 2, electric coupling exists between resonators 1 and 4, magnetic coupling exists between resonators 2 and 3 and mixed coupling exists between resonators 1

and 2 and also between resonators 3 and 4. The positive couplings $M_{12} = M_{21} = M_{34} = M_{43}$ and $M_{23} = M_{32}$ are realized by the mixed and magnetic couplings respectively, while the negative coupling $M_{14} = M_{41}$ is realized by the electric coupling. To confirm that the electric and magnetic coupling coefficients have opposite signs, the transmission phase responses are observed for the two coupling cases. The phase responses are reversed (they are out of phase), indicating that the extracted electric and magnetic coupling coefficients have opposite signs. The coupling coefficients and external quality factors are determined for FBW of 0.06 using (3) and are given below.

$$\begin{aligned} M_{12} &= M_{34} = 0.0514 \\ M_{14} &= -0.0132 \\ M_{23} &= 0.0472 \\ Q_{ei} &= Q_{eo} = 15.9 \end{aligned} \quad (4)$$

The corresponding mutual coupling coefficient matrix for the four-pole edge-coupled bandpass filter is given below.

$$M = \begin{bmatrix} 0 & 0.0514 & 0 & -0.0132 \\ 0.0514 & 0 & 0.0472 & 0 \\ 0 & 0.0472 & 0 & 0.0514 \\ -0.0132 & 0 & 0.0514 & 0 \end{bmatrix} \quad (5)$$

In order to determine the physical dimensions of the filter, full-wave EM simulations are carried out to extract the coupling coefficients and

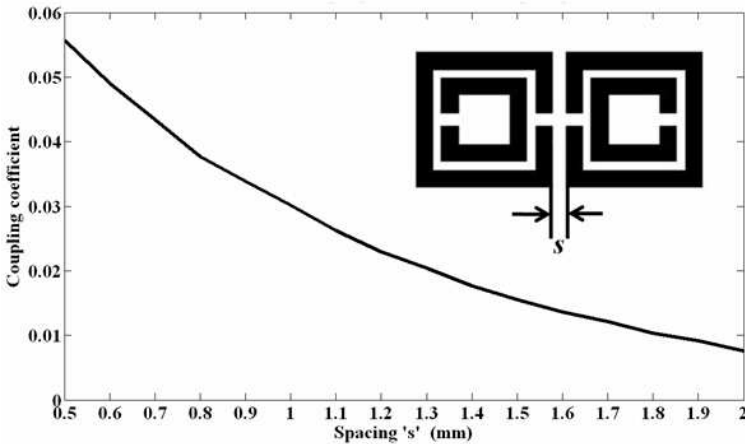


Figure 3. Electric coupling coefficient between resonators 1 and 4 as a function of spacing s between the resonators.

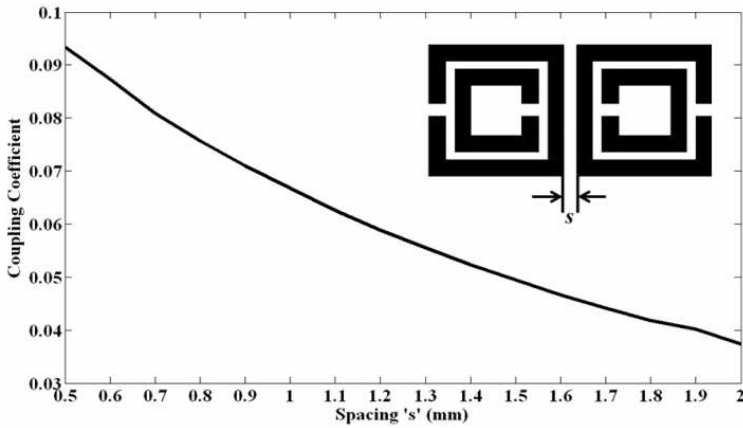


Figure 4. Magnetic coupling coefficient between resonators 2 and 3 as a function of spacing s between the resonators.

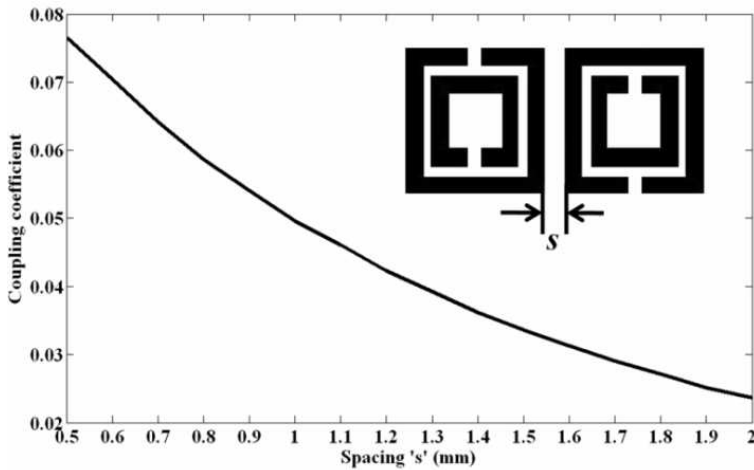


Figure 5. Mixed coupling coefficient for resonators 1 and 2 and also for resonators 3 and 4 as a function of spacing s between the resonators.

external quality factors using the approach described in [25]. For the simulations, the side length of the resonator (L) is chosen to be 16 mm and the conductor width (w) as 2 mm. For each coupling mechanism, a graph is plotted for the coupling coefficient versus spacing. The coupling space ' s ' between the resonators controls the coupling between the resonators and Figures 3–5 show the design curves for the coupling

coefficient plotted as a function of the coupling space 's' between the resonators for electric, magnetic and mixed couplings respectively. The coupling space 's' for the required values of M_{14} and M_{23} can be

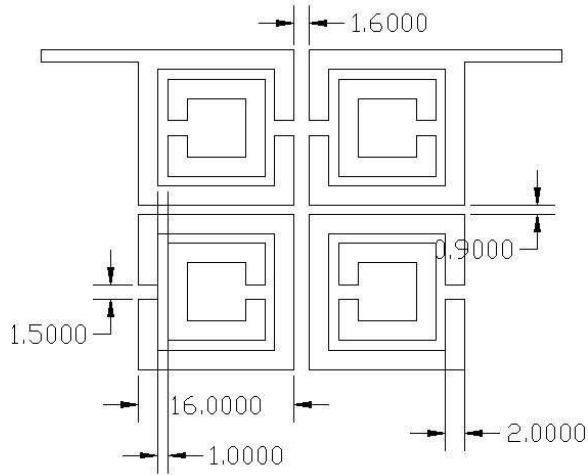


Figure 6. Layout of the final edge-coupled split-ring resonator filter (All dimensions are in mm).

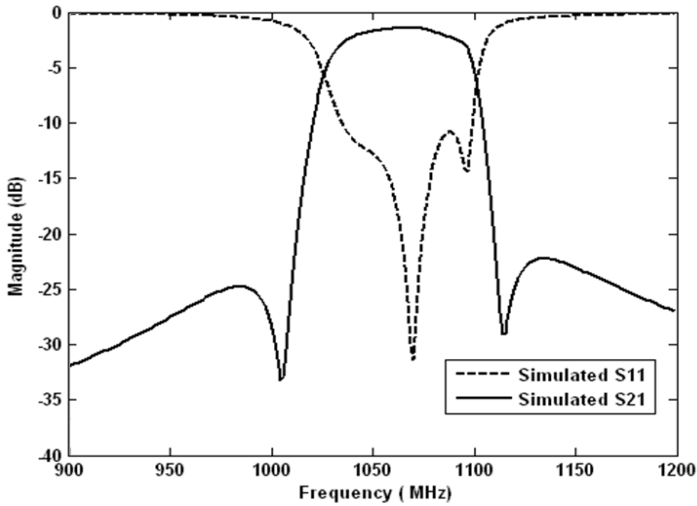


Figure 7. Simulated frequency response ($|S_{21}|_{dB}$ and $|S_{11}|_{dB}$) of the four-pole EC-SRR filter.

determined from Figures 3 and 4 for electric and magnetic couplings respectively and is equal to 1.6 mm. The coupling space 's' for the required M_{12} and M_{34} can be determined from Figure 5 for mixed coupled and is equal to 0.9 mm.

Based on the coupling coefficient matrix, the spacings between the resonators are determined and the final dimensions of the filter are labeled in Figure 6. Width of the feed line is chosen to be equal to 1.192 mm to have $50\ \Omega$ characteristic impedance. The structure is simulated with dimensions shown in Figure 6; the frequency response ($|S_{21}|_{\text{dB}}$ and $|S_{11}|_{\text{dB}}$) of the filter is shown in Figure 7. The passband has a center frequency of 1063 MHz.

The proposed filter is fabricated using a milling machine on RT/Duroid 6010 substrate with relative dielectric constant of 10.2 and dielectric thickness of 1.27 mm and a loss tangent of 0.0023 and the fabricated filter is shown in Figure 8. The circuit size of the fabricated filter is $33.6\ \text{mm} \times 32.9\ \text{mm}$, i.e., approximately $0.119\lambda_0$ by $0.117\lambda_0$, where λ_0 is the free-space wavelength at the center frequency. The frequency response of the fabricated filter is measured with HP8753C vector network analyzer. The measured frequency response of the fabricated four-pole edge-coupled bandpass filter is shown in Figure 9. We can observe from the Figure 9 that the passband insertion loss is about 1.8 dB and the return loss is about 12 dB with fundamental resonant frequency of 1106 MHz and the fractional bandwidth is about 7.5%. The measured results are in good agreement with the simulated results. The frequency shift between the measured and simulated frequency responses is attributed to the fabricated method used (milling machine), assumption of zero metal strip thickness in simulation and possibly because of the deviations in the dielectric thickness of the substrate due to milling.

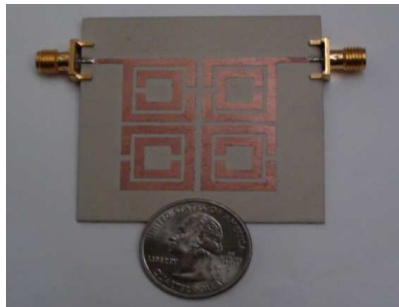


Figure 8. Photograph of the fabricated edge-coupled filter.

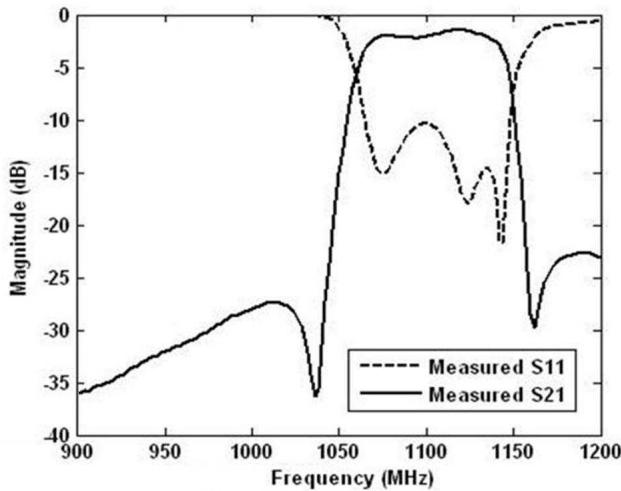


Figure 9. Measured frequency response ($|S_{21}|_{dB}$ and $|S_{11}|_{dB}$) of the fabricated filter.

3. PROPOSED NOVEL BROADSIDE COUPLED STRUCTURE

In this section, a novel two-layered cross-coupled broadside-coupled structure is proposed and the method of extracting coupling coefficient and external quality factor is used to realize the multilayer bandpass filter. Simulation results as well as experimental results are characterized using HP8753C vector network analyzer and comparison to conventional broadside-coupled structure is also presented.

3.1. Conventional Broadside-coupled Resonators

The typical structure of broadside-coupled split-ring resonators (BC-SRRs) is shown in Figure 10. The rings can be either square or circular in shape. Square SRRs are preferred to enhance magnetic coupling [12, 15, 24]. Thus by etching SRRs on both sides of a thin dielectric slab, the distributed capacitance between the rings can be significantly enhanced owing to the broadside coupling [11] which results in a lower resonant frequency compared to the edge-coupled SRRs.

A microstrip filter can be designed using typical BC-SRRs by etching the split-ring resonators on the top-metal layer in close proximity of the feed line and their image (180° inverted) split-rings by etching a window in the ground plane as shown in Figure 11.

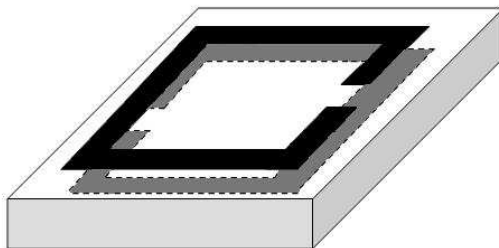


Figure 10. Typical broadside-coupled split-ring resonators (BC-SRRs).

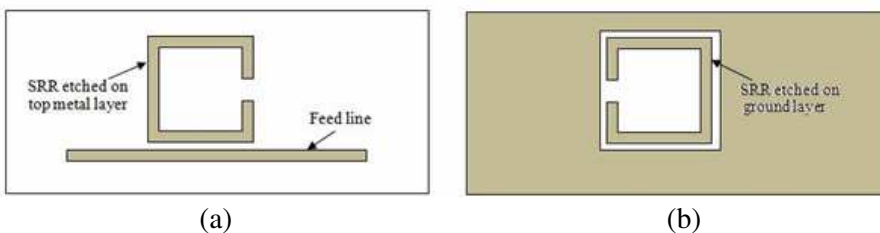


Figure 11. Conventional BC-SRR structure. (a) Top metal layer, (b) ground layer.

The main reasons for realizing BC-SRR structures is to eliminate cross-polarization, bi-anisotropy, and to obtain better miniaturization than edge-coupled SRRs [15]. Higher level of miniaturization can be realized by reducing the thickness of the substrate and thereby increasing the equivalent capacitance of the structure. The substrate should be thin enough for the magnetic flux generated by the current flowing through the feedline to penetrate and excite the SRRs to increase the magnetic coupling between the line and the rings [15].

3.2. New Method for Realizing Multilayer Broadside-coupled Filters

The motivation for moving towards a new method of realizing broadside coupled SRRs is to reduce the resonant frequency to much lower frequencies since there is not much reduction in the fundamental resonant frequency by conventional broadside coupled structure compared to the structure with just resonators etched on metal layer and backed by a ground plane. In [26], a considerable

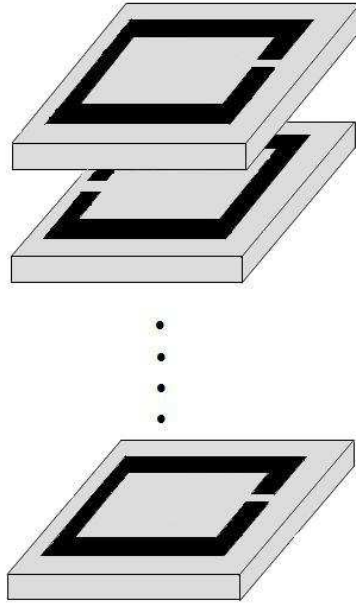


Figure 12. Design idea of multi-layer BC-SRR structure.

reduction in the resonant frequency and high quality factor (Q) were demonstrated for a stack of multi-layer dielectric resonators made of metal strips. The metal strips were used to synthesize an artificial dielectric. This idea is modified to design filters using broadside-coupled SRRs by etching SRRs on multiple layers above the ground plane, with resonators on each layer 180° inverted with than on the other layer to obtain considerable reduction in the resonant frequency for the proposed new structure compared to the conventional broadside-coupled structure.

The preliminary design idea of stacked BC-SRR elements is shown in Figure 12.

In order to verify whether stacking multiple layers with SRRs helps in lowering the resonant frequency, a hollow waveguide loaded with resonators is simulated. Simulations are done by loading the waveguide with a single resonator, two resonators (stacked with metal strips on a dielectric substrate) up to five resonators using the EM software Ansoft HFSS and the resonant frequency for each configuration is observed. For simulation purposes, the side walls are assumed to perfect electric conductors where as the upper and bottom walls are perfect magnetic conductors. The metal strips etched on the dielectric substrate are

assumed to be perfect conductors with a metal strip of width 0.5 mm and side length of 7.8 mm are designed on the dielectric substrate with dielectric constant of 10.2 and height of 1.27 mm as shown in Figure 13.

The resonators on each layer are 180° rotated version with resonators on the other layer, making the configuration as a multi-

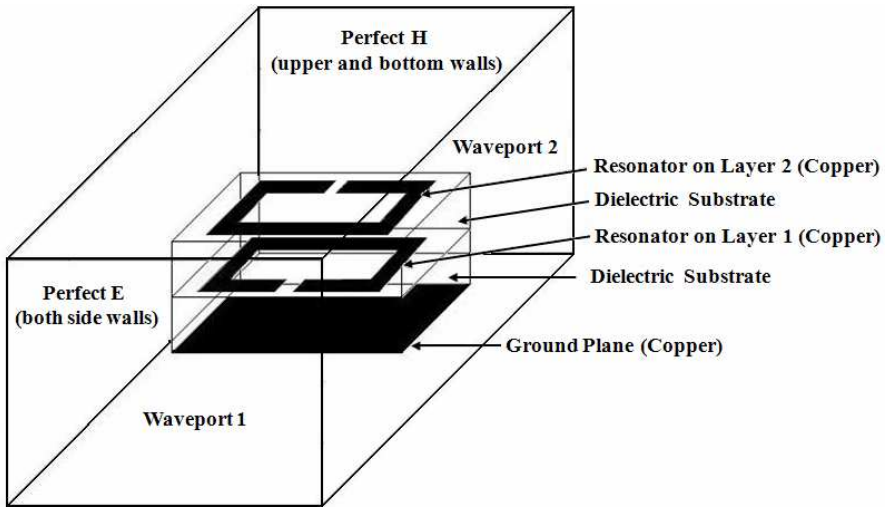


Figure 13. Waveguide loaded with resonators.

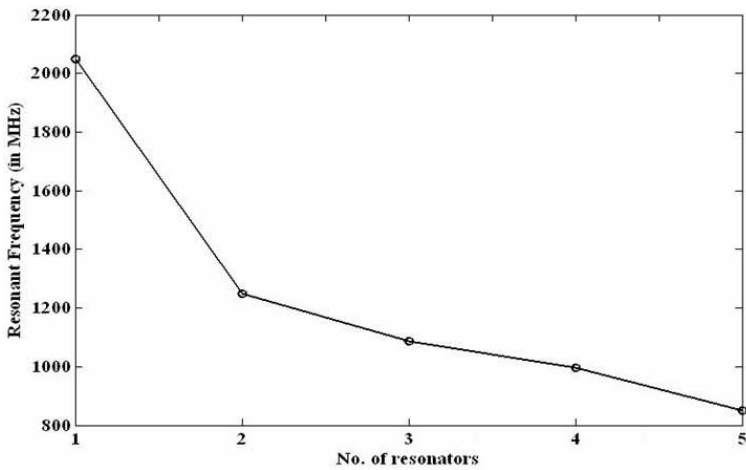


Figure 14. Resonant frequency versus the No. of resonators loaded in waveguide.

layer BC-SRR structure. It has been found that the resonant frequency decreases as the number of stacked resonators increases and the same is shown in Figure 14. The simulation results prove that when the resonators are stacked as shown in Figure 13, the fundamental resonant frequency of the structure is lowered. It is also noted that if either the height of the substrate is reduced or the dielectric constant of the substrate is increased, the resonant frequency can be lowered to a much greater extent. Thus the above simulation results infer that instead of using the conventional broadside coupled structure, if the stacked approach is used in realizing the broadside coupled structure, reduction in fundamental resonant frequency resulting in miniaturized filter structures can be realized.

In this paper, a two-layered broadside-coupled bandpass filter



Figure 15. Proposed two-layered broadside-coupled filter. (a) Bottom layer, (b) top layer.

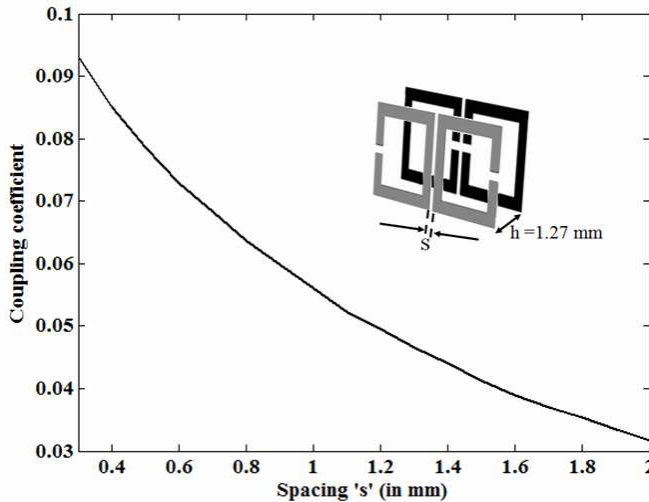


Figure 16. Mixed coupling coefficient as function of coupling space 's' between the resonators.

backed by a ground plane, shown in Figure 15 is realized. In order to determine the physical dimensions of the filter, the method of extracting coupling coefficients described earlier in Section 2 is used.

The side length of the resonator is chosen to be 16 mm and width of the conductor as 2 mm. The same coupling coefficient matrix is used for both filter structures. The coupling coefficients of the three basic coupling structures encountered in this broadside coupled filter were modeled using the approach described in Section 2. In this two-layered

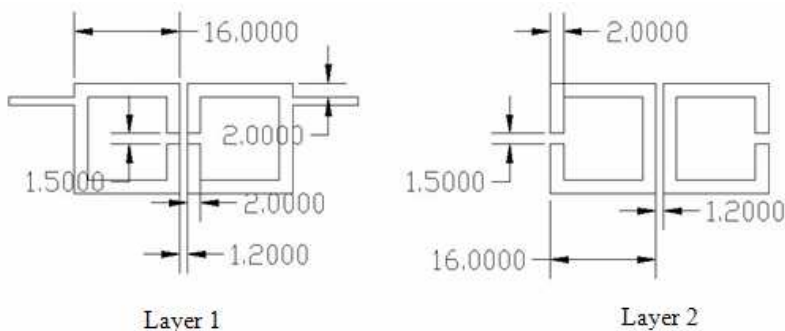


Figure 17. Layout of the proposed two-layer broadside-coupled filter (*dimensions are in mm*).

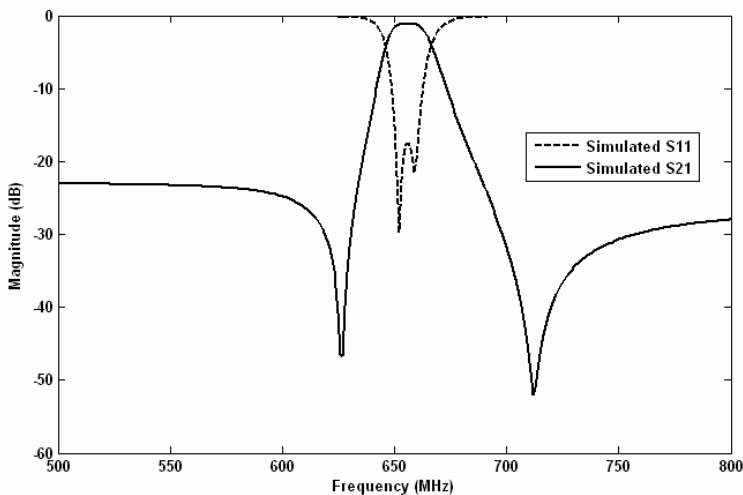


Figure 18. Simulated frequency response ($|S_{21}|_{dB}$ and $|S_{11}|_{dB}$) of the filter.

structure, mixed coupling dominates between the resonators present in layer 1 and layer 2 (Figure 15). The mixed coupling coefficient as a function of coupling spacing ‘ s ’ between the resonators is shown in Figure 16. The coupling space ‘ s ’ for the required mixed coupling coefficient can be determined from Figure 16 and is equal to 1.2 mm.

Final dimensions of the proposed two-layered broadside coupled filter are shown in Figure 17 and simulated ($|S_{21}|_{\text{dB}}$ and $|S_{11}|_{\text{dB}}$) frequency response of the proposed two-layered broadside-coupled filter is shown in Figure 18. From the simulated frequency response of the filter shown in Figure 18, we notice that the center frequency of the filter’s passband is 656 MHz with passband insertion loss of 1.1 dB and return loss of 17 dB.

The proposed two-layered broadside coupled filter is fabricated using a milling machine on a RT/Duroid 6010 substrate with relative dielectric constant of 10.2 and dielectric thickness of 1.27 mm and width of the feedline is chosen to be 1.192 mm to match the $50\ \Omega$ impedance. The photograph of the final fabricated two-layered bandpass filter is shown in Figure 19. The two-layers are attached together using nylon screws. The circuit size of the fabricated filter is 33.2 mm by 16 mm, i.e., approximately $0.073\lambda_0$ by $0.035\lambda_0$, where λ_0 is the free-space wavelength at the center frequency. The fabricated filter was measured with a HP8753C vector network analyzer. The measured frequency response is shown in Figure 20 and the two transmission zeros that are typical of a elliptic function response can be clearly observed.

From Figure 20, we observe that passband insertion loss is about 2.2 dB and a return loss of 13 dB with fundamental resonant frequency of 728 MHz and fractional bandwidth of around 2.5%. From the measured frequency responses (Figures 9 and 20) of the standard EC-SRR and the proposed multilayer BC-SRR, there is 35% reduction in resonant frequency and circuit size is reduced by 50%. Thus, there is

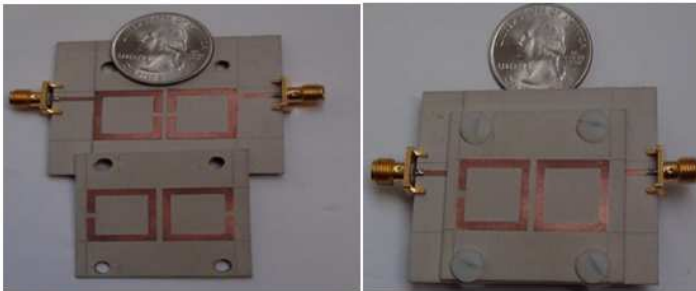


Figure 19. Fabricated two-layered broadside coupled filter.

significant reduction in both the resonant frequency as well as in the size of the proposed multilayer filter.

The frequency shift between the simulated and measured results (Figures 18 and 20) of the proposed multilayer BC-SRR structure is due to the presence of air gap between the fabricated bottom and

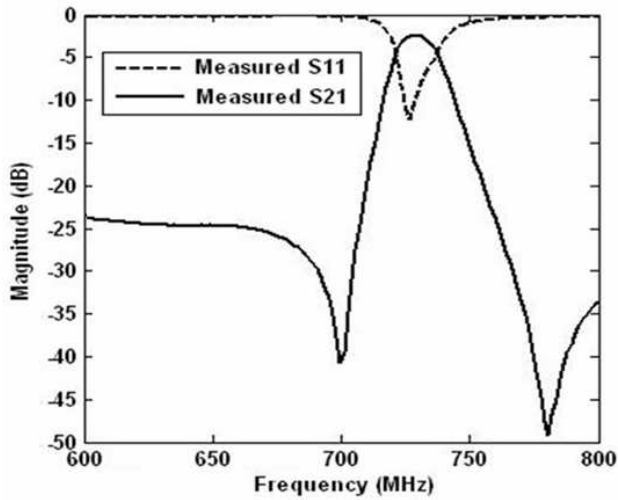


Figure 20. Measured frequency response ($|S_{21}|_{dB}$ and $|S_{11}|_{dB}$) of the fabricated filter.

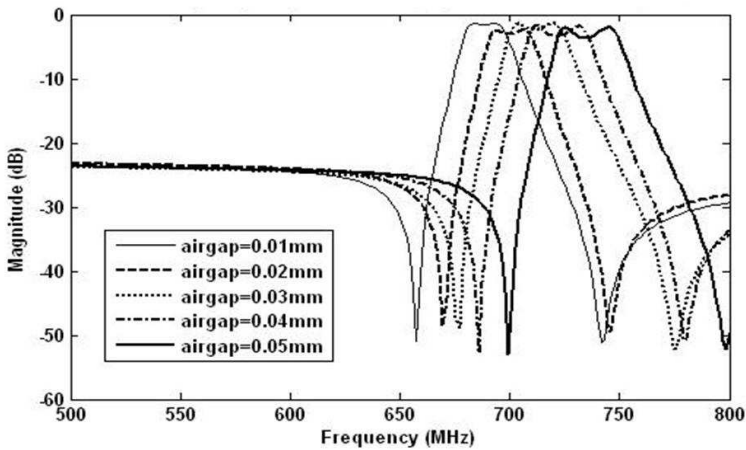


Figure 21. Simulated $|S_{21}|_{dB}$ frequency response with air gap between the layers.

top layers. The air gap between the layers is inevitable when crude fabrication is done by means of a milling machine. To study the effect of the air-gap between the layers, simulations were performed using the EM software Ansoft HFSS. The simulations proved that even a very small air-gap causes a significant frequency shift. Shift in resonant frequency towards higher frequencies with air-gap of 0.01 mm to 0.05 mm between the two layers is shown in Figure 21. Thus, the frequency shift between simulation and measurement results can be eliminated with a better fabrication process, such as the low temperature co-fired ceramic (LTCC) fabrication technology. In addition to higher degree of miniaturization, another advantage of this proposed method is that several layers can be vertically stacked without the need of ground plane or vias or apertures between the resonator layers to achieve coupling.

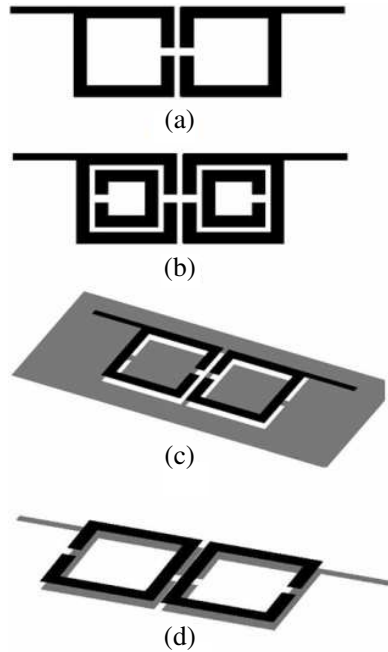


Figure 22. Bandpass filter (a) with open-loop resonators, (b) EC-SRRs, (c) conventional BC-SRRs, (d) proposed two-layered BC-SRRs. ($L = 16$ mm, $w = 2$ mm and $s = 1.2$ mm).

Table 1. Comparison of resonant frequencies for the four bandpass filters.

Bandpass Filter	Resonant Frequency
Open-Loop Resonators (Figure 22(a))	1063.3 MHz
Edge coupled SRRs (Figure 22(b))	1065 MHz
Conventional BC-SRRs (Figure 22(c))	885 MHz
Proposed two-layered BC-SRRs (Figure 22(d), 728 MHz)	656 MHz

3.3. Comparison of Various Bandpass Structures to Illustrate Miniaturization

The level of miniaturization is compared for various bandpass filters using open-loop resonators, edge-coupled split-ring resonators, conventional broadside-coupled resonators and proposed two-layered broadside-coupled resonators. The side-length of all resonators (L) equals to 16 mm, width of the conductor (w) is equal to 2 mm and the separation or coupling space (s) between the resonators is 1.2 mm. In other words, all the four bandpass filter structures have the same circuit size (33.2 mm \times 16 mm). Figure 22 shows the four simulated bandpass filters and comparison of the resonant frequencies for the structures is shown in Table 1.

4. CONCLUSIONS

Microwave filters using single and multilayer coupled resonators were investigated. Most of the previous work on multilayer filters made use of aperture coupling in the ground plane using LTCC and MMIC technologies. The method proposed in this paper eliminates the need for having apertures in the ground plane to achieve coupling among the resonators or vias and resonator layers can be easily stacked. The new method for realizing broadside coupled filters can produce large reduction in resonant frequency compared to the other typical structures. Among the structures presented, the cross-coupled bandpass filter designed using stacked split-ring resonators realized the most miniaturization. There is 35% reduction in the resonant frequency compared to standard cross-coupled EC-SRR structure and

25% reduction in resonant frequency when compared to the single substrate BC-SRR structure. Since a milling machine was used to fabricate the two-layered or stacked structure, air gaps between the two layers are inevitable. The effect of air gap between the multilayered structures on the resonant frequency is also analyzed. Presence of small air gaps can cause significant frequency shift.

REFERENCES

1. Cho, C. and K. C. Gupta, "Design methodology for multilayered coupled line filters," *IEEE MTT-S Digest*, 785–788, 1997.
2. Guan, W. J. and L. A. Carpenter, "A design of vertical coupled stacked bandpass filter using multilayer structure without via," *Proc. Asia-Pacific Microwave Conference*, 2006.
3. Clavet, Y., E. Rius, C. Quendo, J. F. Favennec, C. Person, C. Laporte, C. Zanchi, P. Moroni, J. C. Cayrou, and J. L. Cazaux, "C-band multilayer bandpass filter using open-loop resonators with floating metallic patches," *IEEE Microwave Wireless Components Letters*, Vol. 17, No. 9, 646–648, Sep. 2007.
4. Adam, H., A. Ismail, M. A. Mahdi, M. S. Razalli, A. R. H. Alhawari, and B. K. Esfeh, "X-band miniaturized wideband bandpass filter utilizing multilayered microstrip hairpin resonator," *Progress In Electromagnetics Research*, Vol. 93, 177–188, 2009.
5. Chen, C. F., T. Y. Huang, C. H. Tseng, and R. B. Wu, "A miniaturized multilayer quasi-elliptic bandpass filter with aperture-coupled microstrip resonators," *IEEE Trans. Microwave Theory Tech.*, Vol. 53, No. 9, 2688–2692, Sep. 2005.
6. Tang, C. W., C. W. Shen, and C. C. Tseng, "Design of multilayered broadband bandpass filter with LTCC technology," *Electronics Letters*, Vol. 43, No. 21, Oct. 2007.
7. Hong, J. S. and M. J. Lancaster, "Aperture-coupled microstrip open-loop resonators and their applications to design of novel microstrip bandpass filters," *IEEE Trans. Microwave Theory Tech.*, Vol. 47, No. 9, 1848–1855, Sep. 1996.
8. Bin, Y., "The design of novel multilayer slow-wave aperture-coupled microstrip bandpass filters," *Microwave and Optical Tech. Letters*, Vol. 48, No. 8, 1633–1638, Aug. 2006.
9. Schwab, W. and W. Menzel, "On the design of planar microwave components using multilayer structures," *IEEE Trans. Microwave Theory Tech.*, Vol. 40, No. 1, 67–72, Jan. 1992.
10. Tang, C. W. and H. C. Hsu, "Development of multilayered bandpass filters with multiple transmission zeros using open-

- stub/short-stub/serial semi lumped resonators,” *IEEE Trans. Microwave Theory Tech.*, Vol. 58, No. 3, 624–634, Mar. 2010.
11. Tang, C. W. and D. L. Yang, “Realization of multilayered wide-passband bandpass filter with low-temperature co-fired ceramic technology,” *IEEE Trans. Microwave Theory Tech.*, Vol. 56, No. 7, 1668–1674, Jul. 2008.
 12. Marqués, R., F. Mesa, J. Martel, and F. Medina, “Comparative analysis of edge- and broadside-coupled split ring resonators for metamaterial design-theory and experiments,” *IEEE Trans. Antennas. Propag.*, Vol. 51, No. 10, 2572–2581, Oct. 2003.
 13. Pendry, J. B., A. J. Holden, D. J. Robbins, and W. J. Stewart, “Magnetism from conductors and enhanced nonlinear phenomena,” *IEEE Trans. Microwave Theory Tech.*, Vol. 47, 2075–2084, Nov. 1999.
 14. Smith, D. R., W. J. Padilla, D. C. Vier, S. C. Nemat-Nasser, and S. Schultz, “Composite medium with simultaneously negative permeability and permittivity,” *Phys. Rev. Lett.*, Vol. 84, 4184–4187, May 2000.
 15. Marqués, R., F. Martin, and M. Sorolla, *Metamaterials with Negative Parameters: Theory, Design and Microwave Applications*, Chapter 2, 60–62, Chapter 3, 146–318, New Jersey, John Wiley & Sons, Inc., 2008.
 16. Niu, J.-X., X.-L. Zhou, and L.-S. Wu, “Analysis and application of novel structures based on split ring resonators and coupled lines,” *Progress In Electromagnetics Research*, Vol. 75, 153–162, 2007.
 17. Hasan, A. and A. E. Nadeem, “Novel microstrip hairpinline narrowband bandpass filter using via ground holes,” *Progress In Electromagnetics Research*, Vol. 78, 393–419, 2008.
 18. Matthaei, G. L., L. Young, and E. M. T. Jones, *Microwave Filters, Impedance Matching Networks and Coupling Structures*, Artech House, Norwood, MA, 1964.
 19. Hong, J. S. and M. J. Lancaster, *Microstrip Filters for RF/Microwave Applications*, Chapter 8, 244–258, Chapter 10, 317–320, John Wiley & Sons, New York, 2001.
 20. Wu, G.-L., W. Mu, X.-W. Dai, and Y.-C. Jiao, “Design of novel dual-band bandpass filter with microstrip meander-loop resonator and CSRR DGS,” *Progress In Electromagnetics Research*, Vol. 78, 17–24, 2008.
 21. Dai, G. and M. Xia, “Novel miniaturized bandpass filters using spiral-shaped resonators and window feed structures,” *Progress In Electromagnetics Research*, Vol. 100, 235–243, 2010.

22. Ma, D., Z. Y. Xiao, L. Xiang, X. Wu, C. Huang, and X. Kou, "Compact dual-band bandpass filter using folded SIR with two stubs for WLAN," *Progress In Electromagnetics Research*, Vol. 117, 357–364, 2011.
23. Zhang, J., J.-Z. Gu, B. Cui, and X.-W. Sun, "Compact and harmonic suppression open-loop resonator bandpass filter with tri-section SIR," *Progress In Electromagnetics Research*, Vol. 69, 93–100, 2007.
24. Marqués, R., F. Medina, and R. Rfaii-El-Idrissi, "Role of bianisotropy in negative permeability and left handed metamaterials," *Phys. Rev. B*, Vol. 65, 144440–144446, Apr. 2002.
25. Hong, J. S. and M. J. Lancaster, "Couplings of microstrip square open-loop resonators for cross-coupled planar microwave filters," *IEEE Trans. Microwave Theory Tech.*, Vol. 44, No. 12, 2099–2109, Dec. 1996.
26. Awai, I., "Artificial dielectric resonators for miniaturized filters," *IEEE Microwave Magazine*, Vol. 9, No. 5, 55–64, Oct. 2008.